

AD-A249 261

COPY FOR REPRODUCTION PURPOSES

2

RE

Form Approved
OMB No. 0704-0188

Public reporting burden for this collection of information is estimated to average 1 hour per response, including the time for reviewing instructions, searching existing data sources, gathering and maintaining the data needed, and completing and reviewing this collection of information. Send comments regarding this burden estimate or any other aspect of this collection of information, including suggestions for reducing this burden, to Washington Headquarters Services, Directorate for Information Operations and Reports, 1215 Jefferson Davis Highway, Suite 1204, A

including the time for reviewing instructions, searching existing data sources, gathering and maintaining the data needed, and completing and reviewing this collection of information. Send comments regarding this burden estimate or any other aspect of this collection of information, including suggestions for reducing this burden, to Washington Headquarters Services, Directorate for Information Operations and Reports, 1215 Jefferson Davis Highway, Suite 1204, A

1. AGENCY USE ONLY (Leave blank)		2. REPORT DATE APRIL 7, 1992		3. REPORT TYPE AND DATES COVERED	
4. TITLE AND SUBTITLE EXPERIMENTAL STUDY OF THE SOLID STATE IR VIBRATIONAL LASER				5. FUNDING NUMBERS DAAL03-89-K-0053	
6. AUTHOR(S) A. J. SIEVERS				DTIC S ELEC APR 30 1992 C D	
7. PERFORMING ORGANIZATION NAME(S) AND ADDRESS(ES) CORNELL UNIVERSITY LABORATORY OF ATOMIC AND SOLID STATE PHYSICS CLARK HALL ITHACA, NEW YORK 14853-2501					
9. SPONSORING/MONITORING AGENCY NAME(S) AND ADDRESS(ES) U. S. Army Research Office P. O. Box 12211 Research Triangle Park, NC 27709-2211				10. SPONSORING/MONITORING AGENCY REPORT NUMBER ARO 26383.15-PH	
11. SUPPLEMENTARY NOTES The view, opinions and/or findings contained in this report are those of the author(s) and should not be construed as an official Department of the Army position, policy, or decision, unless so designated by other documentation.					
12a. DISTRIBUTION/AVAILABILITY STATEMENT Approved for public release; distribution unlimited.				12b. DISTRIBUTION CODE	
13. ABSTRACT (Maximum 200 words) During the past grant period the mechanism behind the nonresonant UV pumping of the IR vibrational fluorescence for CN ⁻ in alkali halide crystals has been determined. First an F-center is produced by two UV photon absorption, then the F-center is ionized by another UV photon producing a free electron far up in the conduction band and finally this electron loses its excess kinetic energy by inelastic collisions with the CN ⁻ molecules. This experimental testing of solid state vibrational laser concepts has revealed a new solid state pumping mechanism, namely, the possibility of optically generated conduction electrons preferentially exciting the molecular vibrational modes. In another series of experiments, the low temperature energy relaxation times of the SH ⁻ stretching vibration in five different alkali halide hosts were measured by incoherent laser saturation and by persistent spectral hole-burning and were found to vary from 20 to 250 ps. These times are about 10 ⁸ smaller than previously found for the stretching mode of CN ⁻ in these same hosts. Additional spectroscopic measurements show that the normalized strength of the vibrational sideband for SH ⁻ is roughly equal to that measured for CN ⁻ , suggesting that the dynamical coupling of the stretching mode to phonons, librations, and localized modes is comparable for SH ⁻ and CN ⁻ in contrast with the radically different lifetime measurements. A. J. Sievers/Laboratory of Atomic and Solid State Physics/Cornell Univ./sievers@mac.cornell.edu ajs@helios.TN.CORNELL.EDU/FAX: 607-255-6428					
14. SUBJECT TERMS IR vibrational laser, solid state laser, IR vibrational fluorescence of CN ⁻ , time resolved spectroscopy, vibrational mode relaxation, IR dynamics, nonresonant UV pumping				15. NUMBER OF PAGES 47	
16. PRICE CODE				17. SECURITY CLASSIFICATION OF REPORT UNCLASSIFIED	
18. SECURITY CLASSIFICATION OF THIS PAGE UNCLASSIFIED		19. SECURITY CLASSIFICATION OF ABSTRACT UNCLASSIFIED		20. LIMITATION OF ABSTRACT UL	

EXPERIMENTAL STUDY OF THE SOLID STATE IR VIBRATIONAL LASER

FINAL REPORT

A. J. SIEVERS

APRIL 7, 1992

U. S. ARMY RESEARCH OFFICE

GRANT DAAL03-89-K-0053

CORNELL UNIVERSITY

**APPROVED FOR PUBLIC RELEASE;
DISTRIBUTION UNLIMITED.**

Accession For	
NTIS GRA&I	<input checked="" type="checkbox"/>
DTIC TAB	<input type="checkbox"/>
Unannounced	<input type="checkbox"/>
Justification	
By	
Distribution/	
Availability Codes	
Dist	Avail and/or Special
A-1	



THE VIEW, OPINIONS, AND/OR FINDINGS CONTAINED IN THIS REPORT ARE THOSE OF THE AUTHOR AND SHOULD NOT BE CONSTRUED AS AN OFFICIAL DEPARTMENT OF THE ARMY POSITION, POLICY, OR DECISION, UNLESS SO DESIGNATED BY OTHER DOCUMENTATION.

92 4 28 070


92-11525


Table of Contents

	page no.
I. Summary	1
II. Progress	3
A. Nonresonant UV pumping of the IR vibrational fluorescence from CN^- in Crystals	3
1. Introduction	3
2. Experimental results	4
a. vibrational fluorescence	4
b. UV generated defects	4
c. tracking of F-band and IR fluorescence	6
d. promotion of electron to the conduction band	8
e. UV destruction of aggregation	9
f. fluorescence signatures of visible and UV pumping techniques	9
3. Conclusion: nonresonant UV pumping is a three step process	11
B. Time resolved spectroscopy with fourier transform spectrometers: maintaining the Fellgett advantage	13
1. Introduction	13
2. Background	13
3. Results and Discussion	14
C. Anomalous relaxation of the SH^- stretching mode in alkali halides	17
1. Introduction	17
2. Sideband absorption spectrum of CN^- and SH^-	17
3. Persistent IR spectral hole burning at SH^-	19
4. Incoherent saturation of the SH^- stretch mode	19
5. Lifetime of the SH^- stretch mode vibration in different crystals	22

D. Optical dynamics with the possibility of both slow and fast relaxation processes in solids	25
1. Introduction	25
2. Optical processes involving vibrational solitons	26
E. Laser system to generate picosecond infrared pulses with wavelengths from 1.5 to 8 mm	27
1. Picosecond laser system	27
2. Optical setup for experimental measurements	27
F. Publications, reports and theses (1988-91)	30
G. Participating scientific personnel	38
III. References	39

Table of Contents

	page no.
I. Summary	1
II. Progress	3
A. Nonresonant UV pumping of the IR vibrational fluorescence from CN ⁻ in Crystals	3
1. Introduction	3
2. Experimental results	4
a. vibrational fluorescence	4
b. UV generated defects	4
c. tracking of F-band and IR fluorescence	6
d. promotion of electron to the conduction band	8
e. UV destruction of aggregation	9
f. fluorescence signatures of visible and UV pumping techniques	9
3. Conclusion: nonresonant UV pumping is a three step process	11
B. Time resolved spectroscopy with fourier transform spectrometers: maintaining the Fellgett advantage	13
1. Introduction	13
2. Background	13
3. Results and Discussion	14
C. Anomalous relaxation of the SH ⁻ stretching mode in alkali halides	17
1. Introduction	17
2. Sideband absorption spectrum of CN ⁻ and SH ⁻	17
3. Persistent IR spectral hole burning at SH ⁻	19
4. Incoherent saturation of the SH ⁻ stretch mode	19
5. Lifetime of the SH ⁻ stretch mode vibration in different crystals	22

D. Optical dynamics with the possibility of both slow and fast relaxation processes in solids	25
1. Introduction	25
2. Optical processes involving vibrational solitons	26
E. Laser system to generate picosecond infrared pulses with wavelengths from 1.5 to 8 mm	27
1. Picosecond laser system	27
2. Optical setup for experimental measurements	27
F. Publications, reports and theses (1988-91)	30
G. Participating scientific personnel	38
III. References	39

I SUMMARY

During the past grant period the mechanism behind the nonresonant UV pumping of the IR vibrational fluorescence for CN^- in alkali halide crystals has been determined. First an F-center is produced by two UV photon absorption, then the F-center is ionized by another UV photon producing a free electron far up in the conduction band and finally this electron loses its excess kinetic energy by inelastic collisions with the CN^- molecules. This experimental testing of solid state vibrational laser concepts has revealed a new solid state pumping mechanism, namely, the possibility of optically generated conduction electrons preferentially exciting the molecular vibrational modes.

A new molecule:host system has been uncovered which can make good use of the optically generated conduction electron pumping scheme. We have found that CO_2 molecules trapped in IR transparent chalcogenide glasses have vibrational frequencies appropriate to gas phase modes but without rotation. We are now in a position to use visible bandgap radiation together with an applied electric field to transfer the kinetic energy from the excited conduction electrons to the vibrational modes of the trapped molecules. By introducing both N_2 and CO_2 into the glass, the mechanism of VV transfer can be used to transfer vibrational energy to the molecule of interest in a way similar to its use in the gas phase CO_2 laser. Since the highest frequency vibrational modes are more readily excited by the electrons while the lower frequency modes are more easily relaxed by the phonons the possibility exists that vibrational gain may occur in the solid state in the 10 micron region.

In another series of experiments carried out over the past two years, the low temperature energy relaxation times of the SH^- stretching vibration in five different alkali halide hosts were measured by incoherent laser saturation and by persistent spectral hole-burning and were found to vary from 20 to 250 ps. These times are about 10^8 smaller than previously found for the stretching mode of CN^- in these same hosts. Additional spectroscopic measurements show that the normalized strength of the vibrational sideband for SH^- is roughly equal to that measured for CN^- , suggesting that the dynamical coupling of the stretching mode to phonons, librations, and localized modes is comparable for SH^- and CN^- in contrast with the radically different lifetime measurements. How the short lifetimes for the stretch mode of SH^- in solids at low temperatures can be the same as the times for vibrational modes of molecules in some room temperature liquids is an additional puzzle that needs to be examined in more detail.

We have started experiments with a newly purchased psec tunable IR laser system to carry out pump-probe and photon echo measurements on a number of diatomic and triatomic molecules, with vibrational modes in the 3 to 5 micron region, matrix isolated in solids to provide the first relaxation time survey for small molecules in crystalline solids and glasses. This new ability to tune with short high intensity pulses to IR vibrational transitions will make possible the first systematic investigation of vibrational energy transfer processes while the entire solid remains in the electronic ground state.

II. PROGRESS

A. Nonresonant UV pumping of the IR vibrational fluorescence from CN^- in crystals

1. Introduction

It was discovered near the beginning of this grant that CN^- vibrational emission could be induced by non-resonant UV laser radiation.⁽¹⁾ Since the UV photon energy falls in the transparent region of the host crystal and is not in resonance with any of the electronic states of the CN^- ion, this IR emission is surprising. It was found that the intensity of the CN^- fluorescence depends on the number of laser shots, and is correlated with the growth of the photo-generated color centers (F-centers created by the pump laser) in the sample.

When IR fluorescence spectra were acquired at low temperatures, and on a time scale short compared to the time for energy exchange by CN^- pairs through vibration-vibration exchange, the initial distribution of the vibrational population could be obtained. These spectra show that the excitation of the CN^- ions by the UV pump produces a distribution of vibrational population in the CN^- ions that nearly obeys Boltzmann statistics, with characteristic temperatures on the order of 2300 K ($\sim \hbar\omega_v/k$), much larger than the melting temperature of the host solid but equal to the stretch mode energy. A variety of different kinds of experiments were carried out to determine how the stretch mode was excited and how the apparent "thermal" distribution of vibrational states was obtained. The resultant pumping mechanism is as follows:

- (1) An F-center is formed by two (UV) photon absorption by the laser.
- (2) Subsequently, the F-center is ionized by another UV laser photon producing a free electron far up in the conduction band.
- (3) The free electron loses its excess kinetic energy by inelastic collisions with the stretch modes of a number of CN^- ions and subsequently drops to the bottom of the conduction band.⁽²⁾

The three step pumping mechanism was deduced first by analyzing the IR vibrational fluorescence spectra at short times, these results give us the "initial" vibrational population distribution. Next, it was necessary to determine any correlation between CN^- and UV generated F-centers since it is known that degree of F: CN^- aggregation plays an important role in determining the vibrational fluorescence spectrum. Finally, the UV pump laser wavelength was varied to demonstrate that the UV pumping mechanism is different from the visible pumping in the perturbed F band which had been treated earlier.⁽³⁾ Each of these experiments is now considered in turn.

2. Experimental results

a. vibrational fluorescence

The basic experimental setup⁽²⁾ used to collect the IR fluorescence spectra from CN^- in a variety of alkali halides is shown in Fig. 1. The IR vibrational fluorescence spectrum obtained for $\text{KBr}:\text{CN}^-$ is shown in Fig. 2. A 308 nm XeCl excimer laser is the pump source and the sample temperature is 7 K. The peaks are labelled according to the vibrational quantum number of the upper state of the CN^- internal stretch mode (e.g., the peak labelled 2 is due to the transitions from $v = 2 \rightarrow 1$), and the transitions are separated by the CN^- anharmonic shift of approximately 25 cm^{-1} per level. The monochromator resolution is 10 cm^{-1} ; the emission lines are not spectrally resolved. The spectrum is signal averaged over an interval of 20 μsec . This spectrum represents a snapshot of the fluorescence intensity shortly after the 20 nsec laser pulse.

In analyzing the vibrational fluorescence from alkali halide: CN^- systems, it is important to make the observation time small enough so that vibration-vibration (VV) transfer, which distributes the population among the various vibrational levels, does not have time to occur.⁽⁴⁾ The correct time scale was determined for this case by measuring time resolved spectra with 500 nsec resolution. Spectra were recorded in time bins of 5 μsec duration covering a 45 μsec interval. We found that 20 μsec was the longest time that could be used without VV transfer playing an observable role.

The emission line produced by the $1 \rightarrow 0$ transition in Fig. 2 is distorted and appears to be shifted from its expected frequency. This is caused by ground state reabsorption in the sample. When a CN^- decays radiatively from its $v = 1$ state, the emitted photon is in resonance with the inverse absorption process. Since there are many molecular ions in their ground state, the $1 \rightarrow 0$ emission is reabsorbed. The situation is different for transitions from higher excited states since the density of ions already in the lower excited state is relatively small. These emission lines pass through the crystal unperturbed.

b. UV generated defects

To characterize the different components to the pumping mechanism we next investigate the properties of UV generated defects. The irradiation of alkali halides with an excimer pump laser produces both F and H centers. Once F-centers are present in the crystal, additional UV pumping with the laser produces F center emission. Previous work using psec laser spectroscopy has demonstrated that UV generated F-H pairs are formed within 10 psec, and that F-centers are formed in their ground state.⁽⁵⁾ However, once an F-center is created, direct excitation into the conduction band through the L-bands⁽⁶⁾ is possible. Once in the conduction band

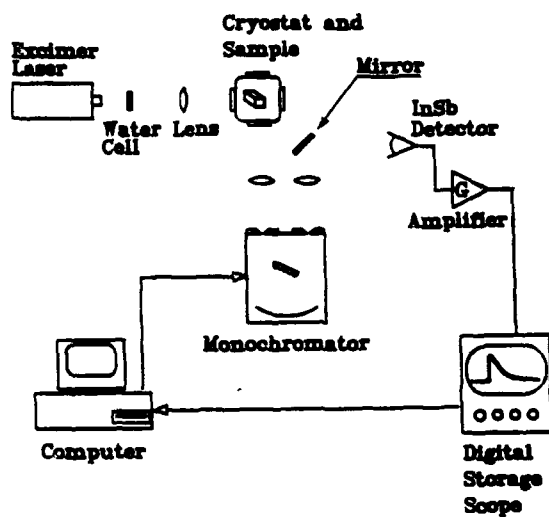


Figure 1. Experimental setup for collecting the UV pumped CN^- vibrational IR fluorescence spectra. The water cell blocks the IR light produced by the laser electronic discharge.

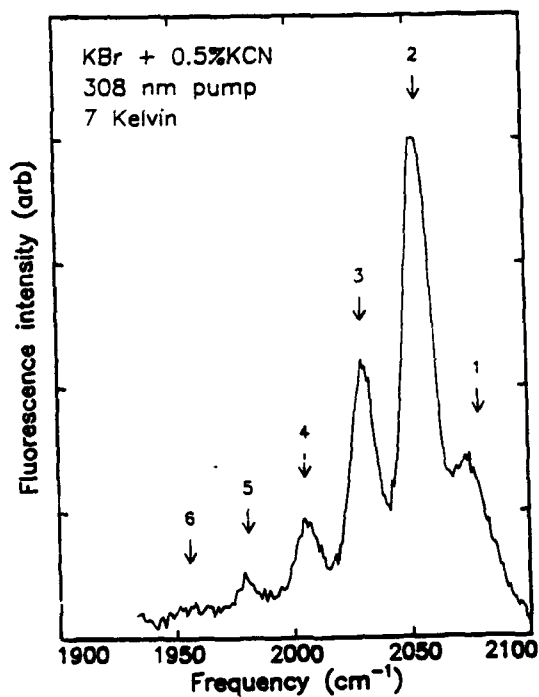


Figure 2. UV pumped CN^- fluorescence spectrum for the KBr host. The spectrum represents an average over the first 20 msec of signal after the laser pump pulse. The emission peaks are labelled according to the upper vibrational level involved in the transition.

then F-band emission readily can be generated as shown by the F-center electron energy level diagram in Fig. 3.

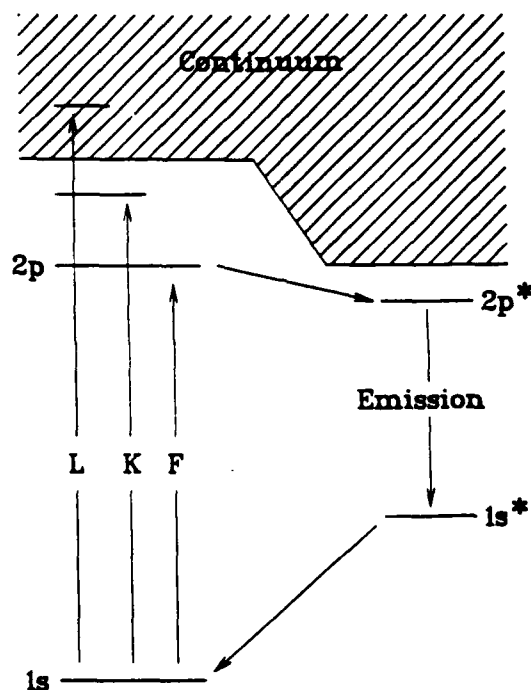


Figure 3. Electronic energy level diagram for the F-center. Optical absorption in the primary F-band promotes the F electron from the $1s$ to the $2p$ state, where it relaxes nonradiatively to the $2p^*$ relaxed excited state, which lies near (~ 0.1 eV) the conduction band edge. From here the electron decays to the $1s^*$ state, emitting a photon which is red shifted relative to the absorption frequency. Subsequent lattice relaxation takes the system back to the $1s$ ground state. The K bands are higher bound excited states outside the conduction band while the L bands are transitions into the conduction band continuum.

c. tracking of F band and IR fluorescence

To identify a connection between the observed defect formation/excitation and the CN^- fluorescence the following experiment was crucial. A fresh sample never previously irradiated and containing no F-centers was pumped at 308 nm, and the F-center and CN^- emission signals were simultaneously monitored as a function of the number of laser shots. Figure 4 shows the results of this measurement.⁽²⁾ Both emission signals grow rapidly with the number of laser shots. As can be seen from the figure the two emission signals track quite closely. The CN^- ground state

reabsorption process, and subsequent non-radiative decay, could account for the small deviation of the CN^- fluorescence growth from that of the F-center. The general result is that there is a correlation between the CN^- fluorescence and the UV generated F-centers.

There are several pieces of information that can be obtained from the results presented in Fig. 4. The zero intercept of the F-center emission growth curve demonstrates that the emission is due to a two step process: F-center formation followed by direct pumping of the F-centers so formed. Note that if the F-center emission were a direct product of the F-H creation process⁽⁷⁾ then the number of excited centers created per pulse is a constant and independent of the number of centers previously created. If the F-center emission was a result of this production process then the emission would be proportional to the defect formation rate. When the resultant intensity is plotted as a function of the number of shots as in Fig. 4, the emission should then be constant, independent of the number of laser shots. The fact that the CN^- emission tracks with the F-center emission shows that the IR pumping process is related to the presence of the F-centers in the crystal, and not to their formation.

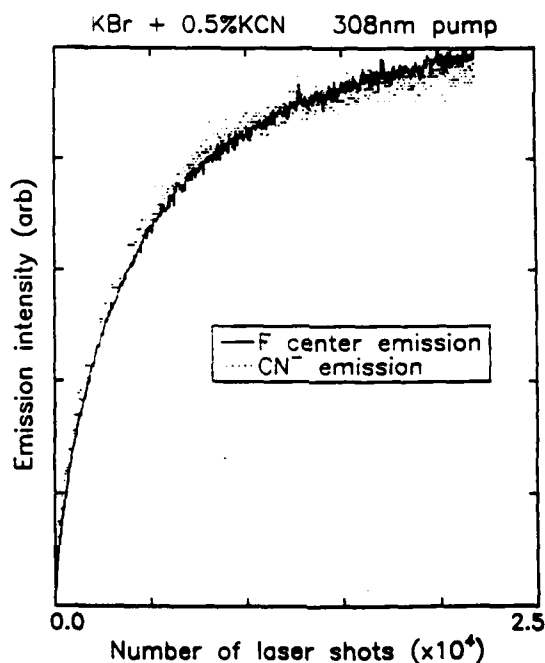


Figure 4. UV pumped CN^- and F center emission growth curves versus the number of laser shots. The solid line gives the F band emission at 1.35 mm, and the dots are the CN^- emission at 5 mm. The sample is at $T = 7$ K.

It should be mentioned that since H centers⁽⁷⁾ are produced at the same time as F-centers there is a possibility that the H center might be the source of the energy transfer to the CN⁻ ion. To test this possibility a crystal was additively colored so that only F-centers were present then the experiment above was repeated. It was found that the CN⁻ emission starts out at a finite level and changed little with UV exposure thus eliminating any H-center mechanism.

d. promotion of electron to the conduction band

We find that the nonresonant pumping of the vibrational fluorescence is turned on between 383 nm and 308 nm. Figure 5 shows the resultant fluorescence spectra for UV pump wavelengths of 383, 308 and 248 nm with the 383 nm shown in the top frame. The IR fluorescence data are

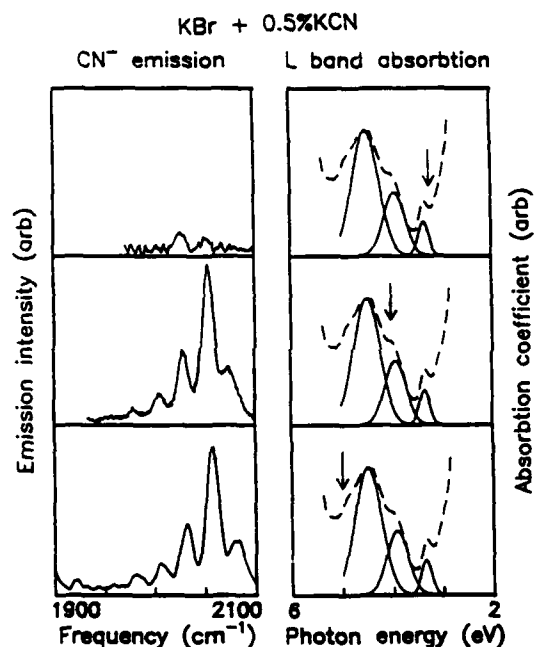


Figure 5. UV pump frequency dependence of the IR emission. The UV pump wavelengths are 383 nm, 308 nm and 248 nm, respectively. The L band absorption in the conduction band is shown at the right with an arrow indicating the photon energy of the pump. The CN⁻ fluorescence spectrum generated is shown at the left. The sample is at T = 7 K.

shown on the left and the conduction band absorption edge including the L bands⁽⁶⁾ on the right. The laser wavelength is identified by the arrows. Similar spectra result from the 248 and 308 nm pumps but very little emission is seen for the 383 nm case. The fact the shortest two laser wavelengths put the electron into the conduction band and give identical spectral results, although

the pump photon energies differ by almost 1 eV, is a clear indication that the conduction electrons play an important role in the pumping process.

e. UV destruction of aggregation

Since F-centers are required to produce IR fluorescence by the UV pumping technique are the important F-centers next to the CN^- ions or randomly distributed in the crystal? To determine the answer to this question F-centers were purposely aggregated with CN^- and the dynamics of these systems studied.^(3,8) KBr:0.5%KCN samples at low temperatures were irradiated with laser light until the F-center density reached saturation in the range 10^{16} to 10^{17} cm^{-3} . The UV generated F-centers were then aggregated to the CN^- ions. The experiment was to pump in the UV while monitoring the CN^- fluorescence spectrum.

Direct optical excitation of the main F-band transition in the visible was used as a probe to gauge the success of the aggregation since the characteristic signature of F: CN^- transfer is strong IR emission on the 3- \rightarrow 2 transition due to the near-resonant transfer of the F-center relaxed excited state into the vibrational mode of the nnn CN^- ion. After achieving aggregation, the samples were pumped with the UV laser for several minutes at 10 Hz. Next the 600 nm dye laser was turned on and the IR fluorescence measured to check for changes in the amount of aggregation. Figure 6 shows the results of this test. The top frame shows the F-band pumped CN^- fluorescence spectrum, with the (3- \rightarrow 2) IR transition serving as a measure of F: CN^- aggregation for a freshly cleaved sample. The second frame shows the resultant IR emission after several more minutes of UV excitation and the third frame, the results after the third excitation period. The effect of the UV laser is to scramble the position of the F-center with respect to the CN^- ion and hence it destroys any aggregation.

f. fluorescence signatures of visible and UV pumping techniques

This contrast between the visible and UV pumping techniques of CN^- can be presented in a different way. Figure 7 shows a comparison of the CN^- fluorescence spectra obtained the 600 nm dye laser pump and the 308 nm UV pump on an aggregated sample. The visible pump preferentially populates the 3- \rightarrow 2 vibrational transition which is the strongest feature in the top frame of this figure.^(3,8) On the other hand the 308 nm pump produces population far up the vibrational ladder.⁽²⁾ No shift is observed for the F-pumped CN^- emission relative to the UV pumped spectrum even though F: CN^- aggregation exists in the former emission spectrum but not in the latter one.

The measured intensity shown in the bottom frame of Fig. 7 when related to the population distribution provides a way to characterize the energy transfer process further. To make this comparison the peak heights of the various transitions are scaled by the quantum number of the

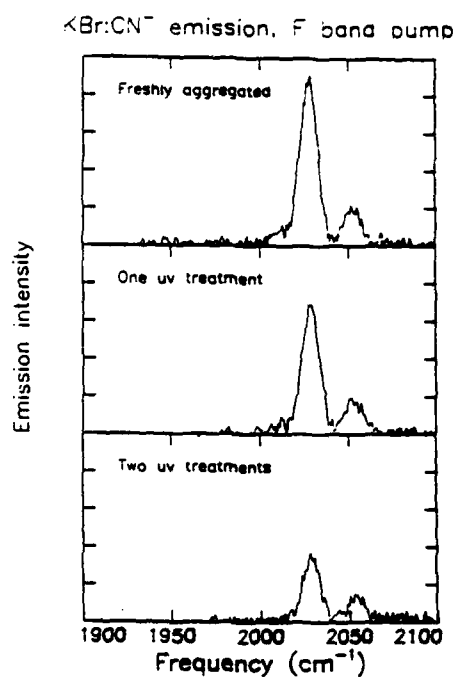


Figure 6. Effect of UV irradiation on the aggregation of the F:CN⁻ pair. As the UV dosage increases more pairs are broken up. The sample is at T = 7 K.

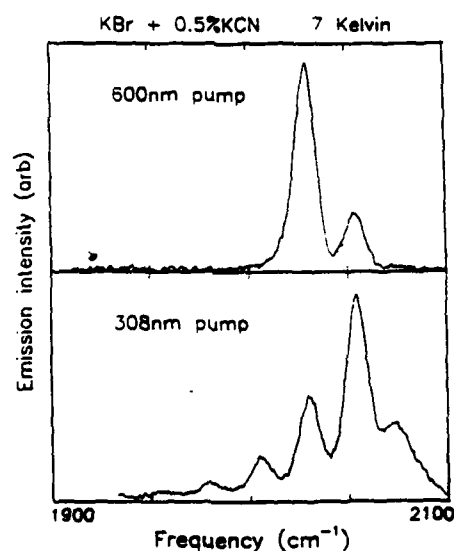


Figure 7. Comparison of the vibrational spectrum obtained by pumping with visible or UV light. Both spectra represent an average over the first 50 msec of signal after the laser pump. The characteristic signal from the F band pump is that the electronic energy is resonantly transferred into the $v = 3$ vibrational level, producing the maximum there. The UV pump transfers energy into a large number of vibrational levels. The sample is at T = 7 K.

upper vibrational state to divide out the square of matrix element and the log of the relative population is then plotted versus the vibrational quantum number. Figure 8 shows that the data can be fit to a Boltzmann distribution. Here the energy spacing between the different levels has been corrected for the 25 cm^{-1} anharmonic shift. The effective vibrational temperature for KBr is 2700 K. Similar vibrational temperatures have been found for CN^- in the other alkali halide hosts.

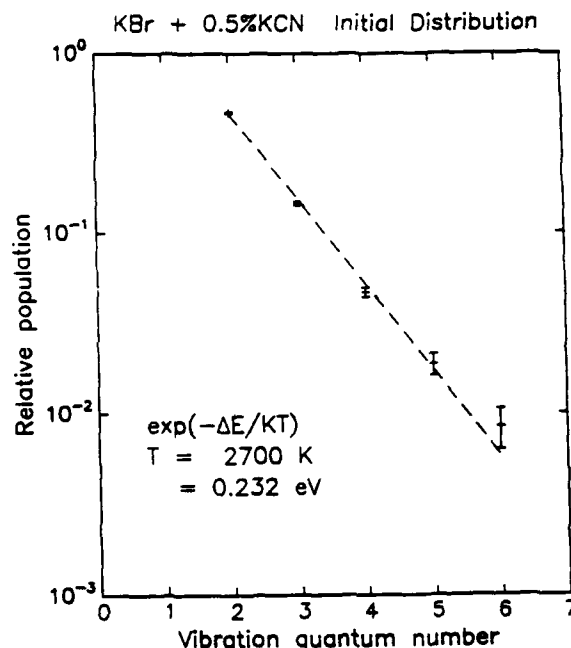


Figure 8. Exponential fit to the initial population distribution produced by a UV pump. The dashed line is a fit to a single Boltzmann exponential with a temperature of 2700 K.

3. Conclusion: nonresonant UV pumping is a three step process

These fits indicate an effective thermodynamic equilibrium between the different stretch modes. Clearly, the fitted temperature is too large to involve the lattice and the time scale of the measurement is too short to make use of VV transfer so it must be the conduction band electrons generated by the UV pump that communicate with the different molecular ions. The dynamical picture is as follows. When the energetic electrons are placed in the conduction band by the L-band pump, they scatter inelastically off the CN^- ions losing one stretch mode quanta of KE energy per scattering event. The initial energy of the electron above the bottom of the conduction band is $\sim 1.3\text{ eV}$ and the CN^- vibrational energy unit is $\sim 0.25\text{ eV}$. After approximately

4 scattering events an electron has an energy equal to the lowest vibrational state and will not be able to get rid of the rest of its kinetic energy by such inelastic scattering. These "cooled" electrons can still run through the lattice, picking up and redistributing the vibrational energy among the CN^- ions. This fast VV transfer process is mediated by these moving conduction electron. The stretch mode degree of freedom for those molecules in contact with the kinetic electrons comes to the same effective temperature as the electrons, namely, $T \sim \hbar\omega_v/k$. When the electrons decay back to the ground state they leave the excited molecular ions frozen at this effective vibrational temperature until at still longer times VV transfer, radiative and non-radiative decay processes come into play.

The conclusion from this work is that the nonresonant pumping occurs because of the following three step chain of events: F-H lattice defect pairs are created by the UV pump, optical ionization of the F electron is produced by the UV pumping of the F-center L band and finally, these energetic electrons in the conduction band transfer most of their kinetic energy into the CN^- vibrational ladder producing the observed IR fluorescence.⁽²⁾

B. Time Resolved Spectroscopy with Fourier Transform Spectrometers: Maintaining the Fellgett Advantage.

1. Introduction

Time resolved spectroscopy (TRS) with FTIR instruments is a developing technique^(9,10) which, in principle, can apply both the Fellgett⁽¹¹⁾ and Jacquinot⁽¹²⁾ advantages to time dependent measurements. At present FTIR instruments which use common optics for both the visible and IR beams, such as the BOMEM DA3 spectrometer, cannot make full use of the Fellgett advantage in time resolved studies. Software has been developed which makes use of multiple scans to collect an interferogram. With this approach the white light (WL) zero path difference (ZPD) signature is used to gauge the absolute position of the scanning mirror once per scan. Hence for interferometers where the infrared and white light beams share common optics, the software can not begin data acquisition until after the infrared zero path difference position. By not collecting the information near the ZPD point, the Fellgett advantage is partially lost. An interferogram with the ZPD region missing will yield the correct line positions and line widths of isolated absorption or emission lines, but broad absorption lines and the relative strength of various portions of the spectrum will be distorted. We have found a simple modification which restores the complete Fellgett advantage for interferometers of this design type.⁽¹³⁾

2. Background

In a scanning FTIR spectrometer, a helium neon laser line is folded into the IR beam path, producing a sinusoidal interferogram as the mirror scans. The zero crossings of this interferogram are used to track the position of the moving mirror to initiate data acquisition at precise sampling intervals. Since the helium neon interferogram cannot identify the absolute mirror position, a broad band white light signal is folded into the IR beam path. The WL interferogram is sharply peaked at the zero path difference (ZPD) position, the point at which the optical path lengths in both arms of the interferometer are identical. A threshold detection circuit is used to monitor the WL interferogram, indicating when the mirror is at the ZPD position, hence it provides a bench mark against which to measure the absolute position of the mirror during the scan.⁽¹⁴⁾

To obtain time resolved spectra with a scanning FTIR spectrometer, an external event must be synchronized with the data acquisition electronics of the FTIR. As an example, consider the specific case of pulsed laser induced IR vibrational fluorescence. In the simplest scenario, the laser output is simply triggered off of the helium neon zero crossings.⁽¹⁵⁾ This approach requires the laser to fire once every sampling interval at a rate determined by the scanning mirror velocity. (316 Hertz for the BOMEM DA3 spectrometer at the slowest practical mirror speed.) If the laser can not

fire at least this fast and/or the system under study relaxes at a slower rate then this direct method will not work.

Software has been developed for the DA3 that circumvents the repetition rate problem.⁽¹⁶⁾ A digital trigger is produced once every N data points, where N is determined by the requested repetition rate. If the sample rate is f Hertz, then the external trigger runs at f/N Hertz. By utilizing the WL ZPD position as an accurate measure of the absolute position of the scanning mirror, the data points skipped on the first scan are filled in during the next N-1 scans. Using this adjustable repetition rate scheme it takes N scans to acquire one complete time resolved interferogram. An additional feature in the software allows the collection of up to 16 interferograms at successive time delays after the trigger pulse.

Although complete in concept, the DA3 optical design limits the Fellgett advantage with the TRS package. The software relies on the WL ZPD signal to position the data points. Since the IR and WL beam paths are identical, the IR and WL ZPD positions are coincident so the first TRS data point occurs just after the IR ZPD causing a portion of the interferogram to be lost. Losing part of the interferogram around the IR ZPD is equivalent to losing the correct overall spectral shape and intensity. In addition, in order to accurately phase correct the interferogram, it should begin well before the ZPD point.

3. Results and Discussion

We have developed an optical method to move the WL ZPD in advance of the IR ZPD so that TRS interferograms can be collected with data acquisition beginning before the IR ZPD. In the DA3, the WL beam occupies the central portion of the combined optical beam; hence, to increase the optical path length of the WL beam relative to the IR beam in the moving mirror arm of the interferometer we introduce an optical retardation plate. The optical delay device is attached with adhesive to the flat surface of the interferometer housing, just below the traveling mirror end point. The central ring holds a 1 inch diameter optical quality glass coverslip approximately 0.15 mm thick. In traversing the coverslip twice, the WL beam acquires an additional $2(n-1)d$ optical path difference relative to the IR beam, where n is the index of refraction and d the thickness of the coverslip. Increasing the WL path length in the moving mirror arm causes the WL ZPD signal to occur before the IR ZPD. The total advance obtained is about 280 periods of the helium neon interferogram, corresponding to a path difference of 177 microns, adequate for performing the phase correction and obtaining undistorted spectra.⁽¹⁶⁾

In order to demonstrate the usefulness of this device in recovering the full Fellgett advantage, an optical shutter is used to simulate a pulsed emission experiment. The shutter is placed in the

sample compartment of the interferometer and operated in a normally closed mode. The TRS external trigger is used to open the shutter. The interferograms and IR spectra obtained with and without the optical path extender are shown in Fig. 9(a,b) and Fig. 9(c,d). The spectra are taken with a KBr beam splitter, HgCdTe detector and globar source. The mirror velocity and shutter trigger rate are set so that it takes 167 scans of the mirror to collect one complete TRS interferogram. As can be seen by comparing Fig. 9(b) and Fig. 9(d), the spectrum obtained with the interferogram missing the ZPD region has the correct position and widths of the sharp features, but the overall shape of the spectrum, and even the polarity of the features is grossly distorted.

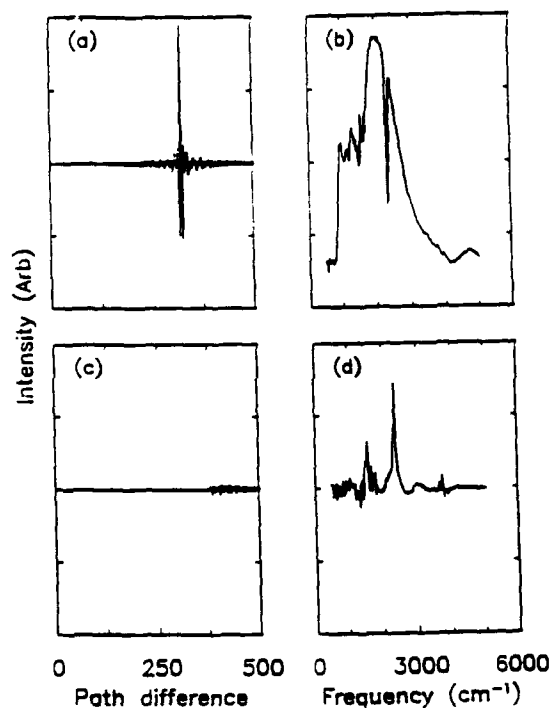


Figure 9. Realizing the Fellgett advantage with the optical path extender. (a) IR interferogram and (b) spectra with WL optical delay. There is sufficient information around the IR ZPD to determine the broad band features of the spectrum. (c) IR interferogram and (d) spectra without WL optical delay. Sharp spectral features come through at the correct locations, but broadband information, and even the polarity of the features, is lost.

As a final illustration of the usefulness of this optical delay technique we show in Figure 10 the time evolution of the IR vibrational emission of the CN^- molecule in KBr after ultra violet excitation with an excimer laser pulse as measured with TRS-FTIR. The uv laser pump generates

an initial distribution of the vibrational population in the electronic ground state of the CN^- molecule. This event is followed by a competition between an up-the-ladder cascade^(4,17) produced by dipole-dipole energy transfer among the CN^- ions and the fluorescent decay from the various anharmonically shifted levels. The various IR transitions seen in emission are labelled in the figure and identified in the figure caption. Note that it would not be possible to obtain these spectra by triggering once per helium-neon interferogram period (3 msec) since the excimer laser has a maximum repetition period of 20 msec and hence cannot fire fast enough to match the sample rate. Even if the laser repetition could be made to match the sample rate, TRS spectra could not be obtained by this triggering technique since the CN^- fluorescence decay is too slow, i.e., it extends over many triggering periods. The BOMEM adjustable repetition rate scheme eliminates this problem.

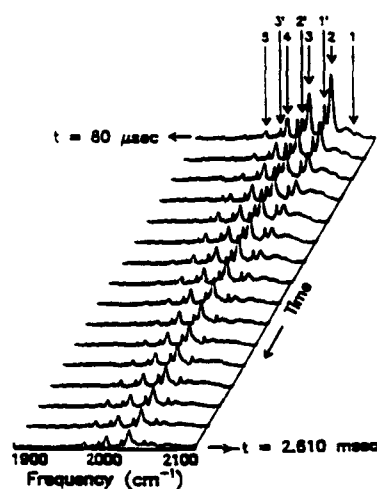


Figure 10. TRS spectra of CN^- IR vibrational fluorescence from the electronic ground state of uv pumped KBr + 0.5%KCN. The pump laser is a XeCl excimer laser running at 12 hertz. The sample temperature is 7 K. The delay from the laser trigger to the first interferogram (here 80 msec) is set independently in software. The time delay (158 msec) between the subsequent 15 interferograms is determined by the mirror velocity. The emission peaks are labeled according to the quantum number of the upper vibrational state of the CN^- anharmonic vibrational manifold, e.g., the peak identified as 2 is from the $v = 2$ to $v = 1$ transition. The primed transitions are from CN^- with the natural abundance of the ^{15}N isotope (the KCN dopant was ^{12}C enriched.). The resolution is 1.5 cm^{-1} . The laser repetition rate is 80 msec and mirror scan velocity is 2 cm/sec. It takes 505 scans to complete one TRS pass (during which all sixteen interferograms are collected). The spectra shown represent the co-addition of five interferograms, with a total run time of 3.5 hours.

C. Anomalous Relaxation of the SH⁻ Stretching Mode in Alkali Halides

1. Introduction

The discovery of infrared vibrational fluorescence from diatomic molecules in solids, first for CO in noble gas matrices⁽¹⁸⁾ and later for CN⁻ in alkali halide hosts^(4,8) showed that at low temperatures radiative dominated nonradiative relaxation. We have carried out experiments on SH⁻ in alkali halides which show for this diatomic that the opposite is true, i.e., it decays nonradiatively, on a 100 picosecond time scale. The fundamental stretching mode of CN⁻ ($\nu_1 \approx 2080 \text{ cm}^{-1}$) relaxes at low temperature in a time on the order of tens of milliseconds,^(19,20) comparable to the radiative lifetime. This accords with the fact that nonradiative multiphonon relaxation processes are very unlikely because of the large number of Debye phonons (roughly 30, depending on the host) required to match the energy of the molecular vibration. We find that the defect-lattice couplings for SH⁻ and CN⁻ are similar, as measured by the strengths of their vibrational phonon sidebands, and thus strong vibrational fluorescence would also be expected for excited SH⁻ defects in alkali halides, especially since the nonradiative decay channel should be even weaker for SH⁻ due to the larger energy of its stretching mode ($\nu_1 \approx 2550 \text{ cm}^{-1}$) and hence to the higher order multiphonon process required. These results are followed by two different kinds of lifetime experiments on the SH⁻ stretch mode, namely, saturation and persistent hole burning which demonstrate that this stretch mode has a very short lifetime in solids.⁽²²⁾

2. Sideband absorption spectrum of CN⁻ and SH⁻

Figure 11 shows the normalized sideband absorption coefficient versus frequency at 1.5 K measured for nominally 0.15 mol % CN⁻ and 0.2 mol % SH⁻ in KI over the frequency interval where it is nonzero. (No other features except the SH⁻ overtone red shifted by 100 cm^{-1} were found in the range $800 - 5600 \text{ cm}^{-1}$). The spectra were normalized by dividing by the appropriate strength of the room temperature vibrational band and then the result was multiplied by the square of the frequency shift⁽²¹⁾ to put the sideband strengths in a standard form so that the integrated sideband areas give a concentration-independent measure of the vibrational coupling to phonons, librations, and local modes. The CN⁻ spectrum is shown in Fig. 11(a); the translational gap mode is at 81.3 cm^{-1} . The zero phonon vibrational lines and the librational mode at 11 cm^{-1} are suppressed by the quadratic frequency term in the normalization. Figure 11 (b) shows the SH⁻ spectrum for comparison; the strongest features here are the isotopic gap modes at 77.0 and 78.3 cm^{-1} . The integrals from 0 to 165 cm^{-1} are 236 cm^{-2} for CN⁻ and 317 cm^{-2} for SH⁻. Both SH⁻ and CN⁻ ion are thus equally strongly coupled to phonons, librations, and gap modes.

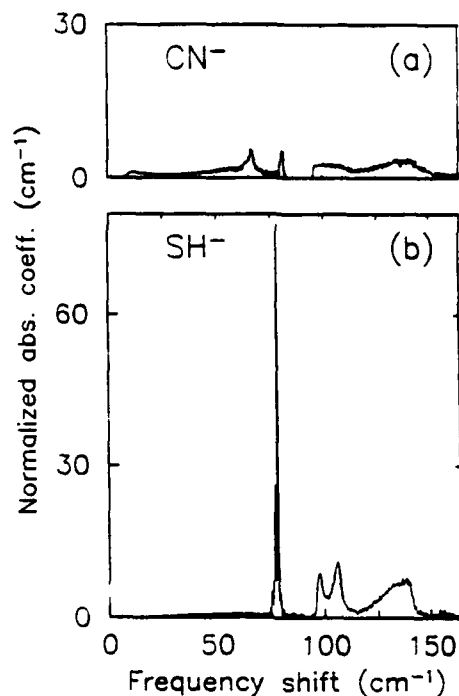


Figure 11. Normalized stretching mode sideband absorption coefficient versus frequency shift from the zero phonon line at 1.5 K and 0.04 cm^{-1} resolution for (a) CN^- and (b) SH^- . The NCO^- lines in the CN^- spectrum have been subtracted out (particularly in the region around 90 cm^{-1}) and the sideband spectrum has been interpolated accordingly in such regions, as depicted. The absorption coefficients have been normalized by multiplying them by the square of the frequency shift and dividing them by the integrated strengths of the fundamental (zero phonon) absorption lines, measured at RT (since they are immeasurably deep at 1.5 K).

In light of this result, one might have expected SH^- to decay mainly radiatively, just as CN^- does. An attempt was thus made to look for vibrational fluorescence. We resonantly pumped the first overtone ($v=0 \rightarrow 2$ transition) of the SH^- molecule in a nominally KI + 0.2 mol % KSH crystal at 1.5 K using a nanosecond infrared laser (with a pulse energy of 3 mJ). An InSb detector was focused to look for fluorescence emitted by the $2 \rightarrow 1$ and $1 \rightarrow 0$ transitions, using an InAs filter to block the scattered pump light. No radiation was detected. Using the noise of the detector as an upper limit for the signal, we calculated an upper limit for the nonradiative relaxation time $< 5 \text{ ns}$. In comparison to the calculated radiative lifetime = 70 ns, nonradiative decay channels clearly dominate the relaxation dynamics of the SH^- stretching mode.

3. Persistent IR spectral hole burning at SH^-

To determine the relaxation time below this upper limit, we used persistent hole-burning and incoherent saturation techniques. Hole-burning measurements, first of all, were performed using a tunable PbEuSeTe double heterojunction diode laser with a focused intensity of up to 2 W/cm^2 . Spectral holes were burned by holding the laser frequency fixed for 3 minutes, then probed by rapidly sweeping the frequency over a few tens of GHz.

We were able to burn persistent holes, with a quantum efficiency of 4×10^{-4} , in the vibrational spectra of SH^- doped into mixed alkali halide crystals. (No persistent holes were observed for SH^- doped into pure crystals.) When 2 mol % KBr was added to KI (to insure inhomogeneous broadening), the main $^{32}\text{SH}^-$ vibrational stretching mode was found to asymmetrically broaden from 0.057 to 0.36 cm^{-1} , and in addition, a second peak, overlapping the weaker $^{34}\text{SH}^-$ isotopic zero phonon line, appeared, which we attribute to a $^{32}\text{SH}^-:\text{Br}^-$ combination mode. Both the asymmetric main line and the combination mode were found to burn, although the former only on its low frequency side, adjacent in frequency space to the combination mode. The antihole was found to extend to higher and lower frequencies just beyond the wings of the hole. The hole FWHM was measured as a function of incident laser intensity; extrapolating to zero intensity gives a width of 1.28 GHz which implies that the dephasing time $T_2 = 500 \text{ ps}$. It also proved possible to burn weak holes in the $\text{SH}^-:\text{Rb}^+$ and the low-frequency side of the asymmetrically broadened SH^- absorption line in $\text{CsI} + 2 \text{ mol \% RbI}$; the hole width gave $T_2 = 740 \text{ ps}$ in this case.

4. Incoherent saturation of the HS^- stretch mode

To make incoherent saturation measurements we have used tunable infrared laser pulses (6 ns pulse length, 0.3 cm^{-1} laser bandwidth, 10 Hz repetition rate, and up to 300 mJ pulse energy), generated around 2550 cm^{-1} by difference frequency mixing of YAG and tunable dye laser radiation in a LiNbO_3 crystal. A small fraction of the pulses were analyzed in a spectrometer to monitor the center frequency and the bandwidth of the radiation. After passing through variable attenuators, the laser pulses were focused onto the SH^- doped samples held at a temperature of 1.5 K . PbSe detectors monitored the incident and transmitted signals and were recorded by a storage oscilloscope.

Saturation of the $\nu = 0 \rightarrow 1$ transition of the SH^- molecule in a KI crystal is evident in Fig. 12. Note that the anharmonic shift is 100 cm^{-1} per ladder level. These spectra have been obtained by sweeping the frequency of the nanosecond laser. At low intensity (top graph), the SH^- stretching mode is responsible for the two absorption peaks near 2559 cm^{-1} . The absorption line is

broadened by the bandwidth of the laser. At high intensity (bottom graph), the absorption has decreased significantly as a result of incoherent saturation of the vibrational transition.

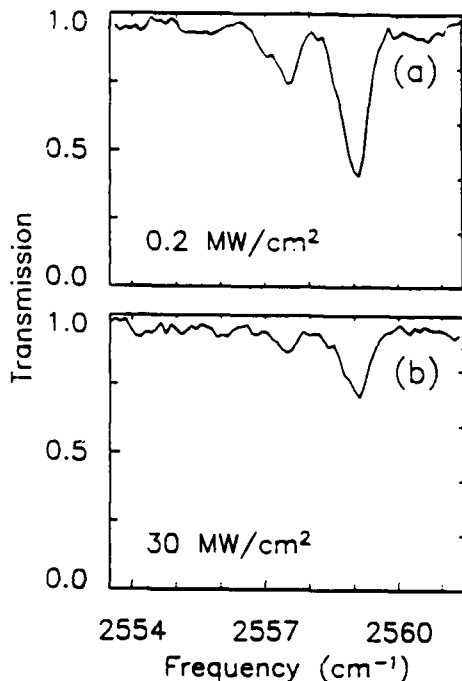


Figure 12. Transmission spectra of a nominally KI + 2 mol % KBr + .02 mol % KSH crystal in the vicinity of the fundamental ($\nu = 0 \rightarrow 1$) transition frequency of SH^- at incident laser intensities of (a) 0.2 MW/cm^2 and (b) 30 MW/cm^2 . The deepest line, at 2559.04 cm^{-1} , is due to the $^{34}\text{SH}^-$ isotope (95% natural abundance); the secondary feature, at 2557.45 cm^{-1} , arises from both the $^{32}\text{SH}^-$ isotope (4.2%) and a $^{34}\text{SH}^-:\text{Br}^-$ combination.

To obtain the saturation parameters for this molecular defect, measurements were made with variable incident laser intensities with frequency tuned to the peak of the SH^- absorption line. Figure 13 shows typical saturation results for SH^- in KI. The experimental points were obtained by measuring the transmission for several hundred laser pulses with different intensities, dividing the intensity axis into bins, and averaging together the data points within each bin. Saturation of the vibrational transition is evident, with an onset at an incident intensity of about 20 MW/cm^2 , and reaches more than 50% overall bleaching at around 300 MW/cm^2 . The saturation curve could not be followed to higher intensities due to resulting crystal damage.

To analyze the saturation data, it can be assumed that a nearly identical relaxation time T_2 would be found for SH^- in a pure host and in one to which 2% of another alkali halide has been

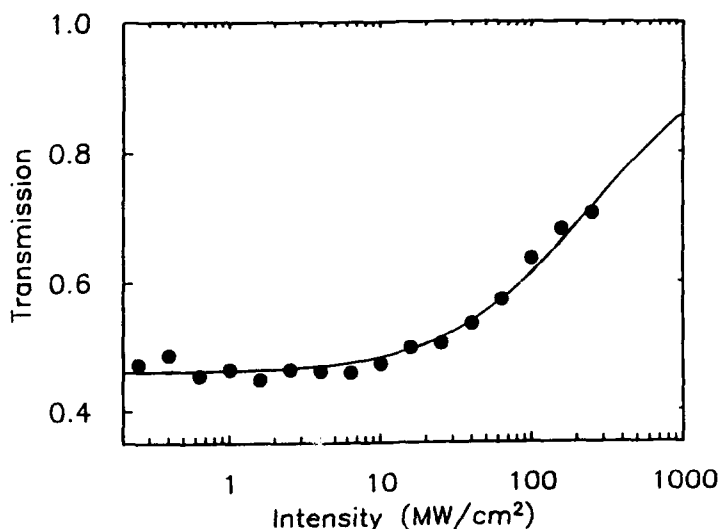


Figure 13. Transmission of a nominally KI + 60 ppm KSH sample as a function of the incident intensity of laser radiation resonant with the stretching mode, ν_1 . Experimental data are indicated by the dots, and the solid line using a rate equation analysis with $T_1 = 100$ ps.

mixed in.⁽²²⁾ The homogeneous linewidths calculated from the spectral hole widths for the mixed crystals are comparable to those measured for the pure hosts by ordinary absorption spectroscopy (see Table 1). Thus, the hole-burning results imply that the lines are almost homogeneously broadened. Hence, in the following analysis we can assume, with only slight error, that the absorption lines are homogeneously broadened.

Owing to the large anharmonic shift⁽²³⁾ of 100 cm^{-1} in the vibrational ladder of SH^- , the incident radiation is only resonant with the $\nu = 0 \rightarrow 1$ transition, so that the molecule can be treated as a two level system. In our experiments, the laser bandwidth exceeds the absorption linewidth by about a factor of 3, so that, to a good approximation, we can regard the vibrational transition as a two level system exposed to a radiation field of constant spectral intensity. We have then applied a standard rate equation analysis⁽²⁴⁾ to compute the transmitted intensity as a function of the incident intensity, numerically integrating over the transverse (assuming a Gaussian beam profile) and longitudinal coordinates as the laser pulse propagates through the crystal. The final result depends upon the integrated absorption cross section of SH^- , the value of which was determined by performing a chemical analysis⁽²³⁾ to find the actual SH^- concentration in a crystal and dividing this into its measured absorption strength. Next, the value of the energy relaxation time T_1 for each host was varied until a best fit to the experimental data was found; for example, the fitted saturation curve for nominally KI + 60 ppm KSH is presented in Fig. 13.

5. Lifetime of the SH⁻ stretch mode vibrations in different crystals

The results of the fits are plotted in Fig. 14 for five different hosts, together with the corresponding lifetimes for CN⁻ from Ref. 20. (For the case of KCl, no definitive saturation could

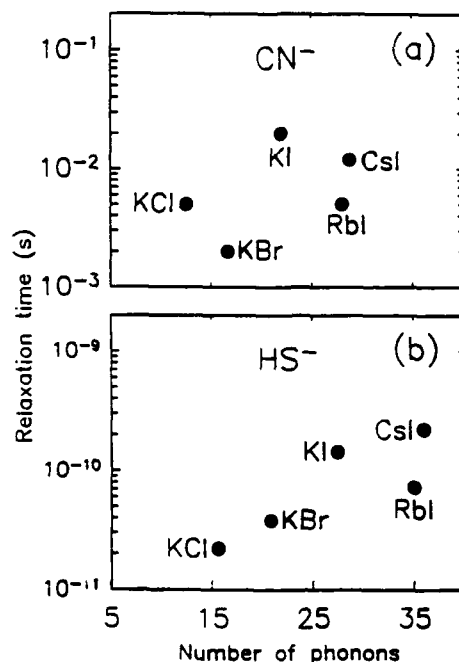


Figure 14. Energy relaxation times T_1 of the vibrational stretching mode in five different hosts for (a) CN⁻ (from Ref. 20) and (b) SH⁻. Note the 8 orders of magnitude faster relaxation for SH⁻ than for CN⁻ in the same hosts.

be observed. From this, we find an lower limit on the relaxation time of 20 ps, as listed in Table 1; the upper limit of 48 ps is determined by the measured 0.11 cm⁻¹ absorption linewidth.) The fitted values for T_1 agree, to within errors, with the values found from hole-burning for KI and CsI, assuming that energy relaxation dominates so that pure dephasing can be neglected, implying $T_2 = 2T_1$. We thus find a difference in the relaxation times of seemingly similar molecules, SH⁻ and CN⁻, of eight orders of magnitude (note that the data for CN⁻ were obtained at 80 K; at 1.5 K the relaxation times would be even longer). The horizontal axis in the figure gives the number of Debye phonons, ν_1/ν_D (where ν_D is the Debye frequency), which is required to pick up the vibrational energy. There seems to be a trend for both SH⁻ and CN⁻ that the relaxation time decreases with decreasing number of phonons, although it is unclear what causes the great difference in the relaxation times of SH⁻ and CN⁻.

Besides examining the CN⁻ stretch mode lifetime in the same host there is another kind of

comparison that one can make to demonstrate the anomalous character of the SH^- relaxation time. The relaxation times of some molecules in liquids at room temperature have been measured over the last few years. For nonassociated solvents like CCl_4 the room temperature vibrational lifetime for the CH stretch^(25,26) of bromoform (CHBr_3) in the liquid is 40 to 55 ps, the same order of magnitude as the values given in Table 1 for SH^- in an ordered solid at 1.7 K. When viewed from this perspective it again seems unlikely that the usual phonon decay mechanism should be invoked to explain the rapid relaxation of the SH^- stretch mode in the solid state.

In conclusion, we have performed persistent hole-burning and incoherent saturation experiments on the fundamental stretching vibration of SH^- molecules in alkali halide hosts. We find that the energy relaxation times are about 8 orders of magnitude shorter than the corresponding times for CN^- , a result that cannot be explained by standard models of nonradiative decay into phonons and localized modes.

Table 1. Comparison of measured and calculated linewidths at 1.5 K for SH^- doped in the indicated host crystals at low concentrations. The second column gives the linewidths (for unmixed hosts) measured using a Fourier transform interferometer; the 0.04 cm^{-1} resolution has been deconvolved from the tabulated values. The third column gives the fitted values of T_1 from the saturation curves, as explained in the text; the tabulated values are the averages of several runs using different boules. These values have been used to calculate the homogeneous linewidths listed in the fourth column. Another measure of the homogeneous linewidths is given by half of the spectral hole FWHM, γ_{hole} , as tabulated in the fifth column, and obtained by double-doping with SH^- and 2 mol % of a second alkali halide, as explained in the text. The linewidths measured by absorption spectroscopy are comparable to those determined by the saturation and hole-burning techniques; hence, we conclude that the lines are mainly homogeneously broadened, with perhaps a slight amount of random strain broadening.

host	linewidth (cm^{-1})	fitted T_1 (ps)	$1 / 2\pi T_1$ (cm^{-1})	$\gamma_{\text{hole}} / 2$ (cm^{-1})

KCl	0.11	20	0.27	-
KBr	-	40	0.13	-
KI	0.041	140	0.038	0.021
RbI	0.091	65	0.082	-
CsI	0.038	230	0.023	0.014

D. Optical dynamics with the possibility of both slow and fast relaxation processes in solids

1. Introduction

Although the plane wave description of vibrational modes in a perfect lattice, originated by Debye to account for the low temperature specific heat of solids, is a corner stone of solid state physics it does not completely characterize the vibrational dynamics of all systems, e.g., glasses.⁽²⁷⁾ Recently, it was proposed that this plane wave description of solid state vibrational modes does not provide a complete description even for a weakly anharmonic lattice since in some instances inhomogeneous (or localized) wave solutions can occur.⁽²⁸⁻³²⁾

These new vibrational modes can be demonstrated by adding a hard quartic potential to the harmonic one in a monatomic lattice with nearest neighbor springs. If the quartic term or the particle amplitude is large enough, then self-localized modes of an optical character appear above the top of the plane wave spectrum.⁽²⁸⁻³²⁾ They can be thought of as a new kind of soliton with optical character.

Computer simulation studies⁽³¹⁻³⁵⁾ by a number of groups have shown that the anharmonic localized mode is stable, that it exists in any dimensions and that the eigenvector of such a localized excitation is orthogonal to the remaining plane wave modes. Hence the total number of normal modes of the system remain the same but now some are plane wave and some are localized.

This mixed mode picture gives a new format with which to describe the vibrational dynamics and hence energy transfer in solids. For example, under certain initial conditions such anharmonic systems could be bistable. To see this, one must recognize that the plane wave description minimizes the anharmonic contribution in the vibrational mode. The resultant amplitude in a mode is made up from the contributions summed over all potential sites, N , so at any particular site the rms amplitude is extremely small, on the order of $(N)^{-1/2}$. Such a small amplitude mainly probes the harmonic part of the potential. The local mode (or Einstein oscillator) picture, on the other hand, maximizes the anharmonic contribution in the mode since now only a few atoms are vibrating hence each must have a much larger amplitude to account for the same degree of freedom as in the previous case. Such large amplitudes probe the quartic potential.

One possible result of this vibrational dichotomy is that at low temperatures the vibrational dynamics could be completely described by the plane wave picture (Debye) but as the rms amplitude increases with temperature, the available configurational entropy would permit localized (Einstein) modes to be produced at the expense of the plane wave (Debye) modes.

2. Optical processes involving vibrational solitons

Another possibility is that a large amplitude disturbance at a particular site in the crystal such as that produced by a Mössbauer recoil or an optical, UV or X-ray excitation process could create these localized anharmonic modes. Moreover, with the addition of impurities to the crystal, self-localized modes could be trapped at defects in anharmonic crystals at low temperatures but, in contrast with the behavior of "standard" harmonic impurity modes which remain fixed at the impurity site, they could be "released" into the perfect lattice at high temperatures. An attempt to describe the energy transfer processes in terms of the standard harmonic lattice dynamics picture (without self-localized modes) would produce apparently anomalous results.^(36,37)

Independent of whether or not self-localized modes will provide the correct description of energy transfer processes, it has become evident in the past few years that in many cases the observed energy transfer from excited optical centers to the solid is not consistent with the underlying assumptions of known dynamical mechanisms such as multiphonon decay.

The new IR psec laser system permits tunable pump-probe measurements to be made of the vibrational modes of molecular and point defects in a variety of solids. This equipment will permit vibrational energy transfer studies on a great many more molecular systems. To date we have made use of a few accidental coincidences of fixed frequency gas laser lines with vibrational modes in order to determine how the "Q" of the normal modes of molecules, as large as $\sim 10^{10}$ in the gas phase, was affected by different solid state surroundings. In a couple of cases this coincidence has made possible a detailed probing of the energy transfer from the vibrational degrees of freedom to the host lattice.

The laser system generates picosecond infrared pulses with wavelengths from 1.5 to 8 μm . It consists of a high-energy mode-locked Nd:YAG laser, part of whose output is doubled and used to pump a set of picosecond dye laser stages. Infrared generation is achieved by mixing the dye laser output with the residual YAG fundamental in a nonlinear crystal. This ability to tune a high intensity picosecond source to IR vibrational transitions will make possible the first systematic investigation of energy transfer processes between vibrational degrees of freedom and the lattice modes while the molecule remains in its electronic ground state.

E. Laser system to generate picosecond infrared pulses with wavelengths from 1.5 to 8 μm .

A recently purchased laser system is being set up in the laboratory which generates picosecond infrared pulses with wavelengths from 1.5 to 8 μm . It consists of a high-energy mode-locked Nd:YAG laser, part of whose output is doubled and used to pump a set of picosecond dye laser stages. Infrared generation is achieved by mixing the dye laser output with the residual YAG fundamental in a nonlinear crystal. The components are as follows.

1. Picosecond Laser System

The PY61C-10 from Continuum is a high-energy actively and passively mode-locked Nd:YAG laser. By cavity dumping the oscillator, single pulses with a width of 20 psec can be extracted at a repetition rate of 10 Hz. After passing through a high gain amplifier, pulses with an energy of 50 mJ are obtained. Due to the high peak power, doubling in the model D second harmonic generator results in 25 mJ and 10 psec pulses at 532 nm. A wavelength separator model WSP-1A is used to separate the second harmonic output from the 20 mJ residual fundamental of the YAG laser.

The second harmonic of the YAG pumps a PD10 picosecond dye laser system, which produces tunable narrow-band visible and near IR radiation. This laser system uses a short oscillator to create single-mode pulses with temporal widths of less than 10 psec. Two amplifier stages boost the energy of these pulses to between 100 and 800 μJ in the region 700 - 940 nm and 1 to 5 mJ between 580 and 700 nm. The single-shot linewidth is about 5 cm^{-1} , which can be decreased however to about half of this value by inserting a narrow-band filter between the dye oscillator and the amplifier stages. The PD10 system includes an automatic stabilization mechanism which keeps the integrated width of these pulses roughly comparable with the single-shot value.

After spatially filtering the dye and the residual YAG fundamental laser beams, difference frequency mixing occurs in a nonlinear crystal. Below 4 μm , LiNbO_3 will be used; at longer wavelengths, AgGaS_2 must be used instead. Typical final output pulse energies exceed 10 μJ . The bandwidth is dominated by the dye laser linewidth and is about three times the transform limit. An external Fabry-Perot etalon can be used, if necessary, to reduce this linewidth.

2. Optical setup for experimental measurements

The output pulses are used for pump-probe or photon echo measurements of the mid-infrared modes of molecular impurities in crystals and glasses. For this purpose, it is necessary to split the output pulses into a pump and a probe beam, which are subsequently focused onto a sample

suspended in a variable temperature cryostat and detected using a sensitive detector. This requires the experimental setup shown in Fig. 15.

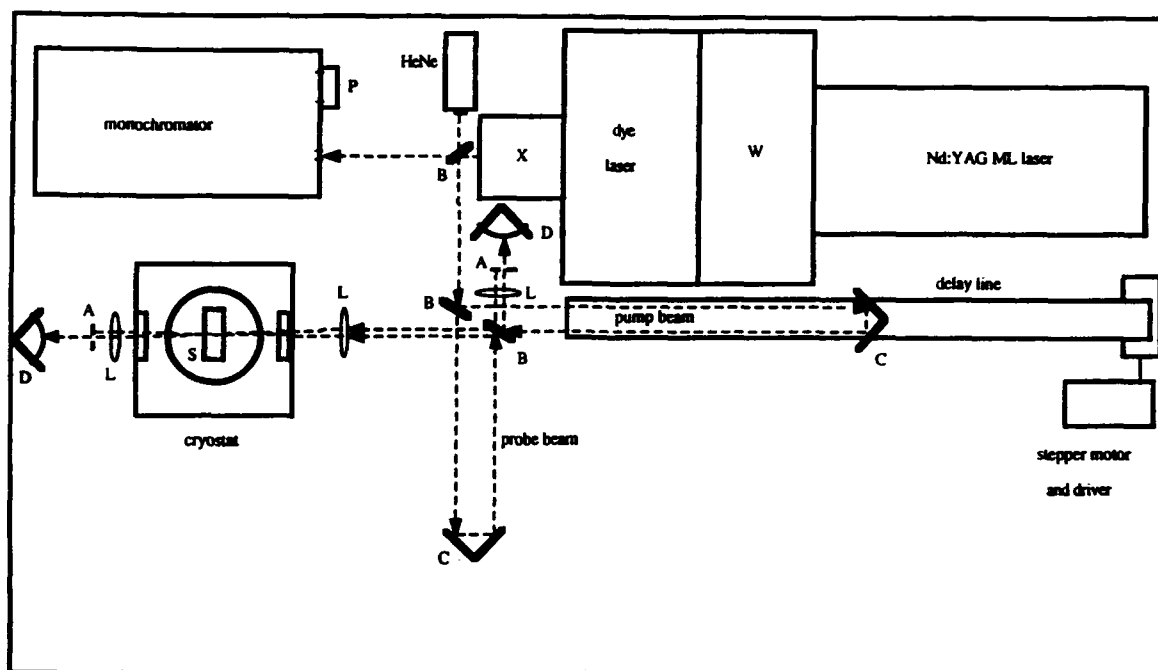


Figure 15. Setup for IR tunable picosecond laser system. The dashed lines indicate the optical path. The letters identify the following components: A = aperture, B = beamsplitter, C = corner-cube retroreflector, D = MCT detector, L = lens, M = mirror, P = PbSe array detector, S = sample, W = second harmonic generator and wavelength separator and X = difference frequency mixing module.

The output laser beam from the picosecond laser system is split using a beamsplitter into a high energy pump beam and a weak probe beam. The probe beam is delayed with respect to the pump beam, using a corner cube mounted on a precision 72-inch long motorized translation stage, which will be computer-controlled using a stepper motor and driver. The two beams are subsequently brought back into near-parallelism and directed onto the sample.

A low temperature optical access cryostat is used to cool the samples to between 1.5 and 300 K to study the temperature dependence of the relaxation processes. Visual access is provided through a set of BaF₂ indium-sealed windows which are transparent to the IR laser pulses.

A liquid-nitrogen-cooled MCT detector is used to detect the signals transmitted through the sample. This detector is useful in the range 2 to 12 μm .

Beam diagnostics are obtained by splitting off small fractions of the laser beam. A high-resolution monochromator is used to monitor the peak frequency and bandwidth of each individual pulse. An array of ten PbSe detectors simultaneously monitors the frequency components of any given pulse. Finally, the pulse energy incident on the sample is determined by using a reference detector which is identical to the signal detector.

F. Publications, reports and theses (1988-91)

(Note: A \oplus in front of the publication indicates that the work was supported by ARO.)

- \oplus "Persistent Changes in the FIR Spectrum of $\text{KI}:\text{NO}_2^-$ Produced by IR Vibrational Hole Burning," W. P. Ambrose and A. J. Sievers, *Chemical Physics Letters* **147**, 608 (1988).
- \oplus "Intrinsic Localized Modes in Anharmonic Crystals," A. J. Sievers and S. Takeno, *Physical Review Letters* **61**, 970 (1988).
- \oplus "Anharmonic Resonant Modes in Perfect Crystals," S. Takeno and A. J. Sievers, *Solid State Communications*, **67**, 1023 (1988).
- "Optical Reflectivity Studies of Polycrystalline LaBaCuO and LaSrCuO ," S. G. Kaplan, T. W. Noh, P. E. Sulewski, H. Xia, and A. J. Sievers, *Physical Review B* **38**, 5006 (1988).
- "The Far Infrared Absorptivity of UPt_3 ," P. E. Sulewski, A. J. Sievers, M. B. Maple, M. S. Torikachvili, J. L. Smith and Z. Fisk, *Physical Review B* **38**, 5338 (1988).
- "Microwave Superconductivity for Particle Accelerators - How the High T_c Superconductors Measure Up," H. Padamsee, K. Green, J. Gruschus, J. Kirchgessner, D. Moffat, D. L. Rubin, J. Sears, Q. S. Shu, R. Buhrman, D. Lathrop, T. W. Noh, S. Russek, and A. J. Sievers, *Conference on Superconductivity and Applications, Institute on Superconductivity, SUNY Buffalo, April 18-20, 1988.*
- \oplus "Isotope-shift measurement of the NO_2^- gap mode spectrum in KI with persistent IR spectral holes", W. P. Ambrose and A. J. Sievers, *Physical Review B* **38**, 10170 (1988).
- \oplus "Intrinsic Localized Vibrational modes in Anharmonic Crystals," S. Takeno, K. Kisoda and A. J. Sievers, *Progress in Theoretical Physics, Supplement* **94**, 242 (1988).
- \oplus "Persistent Infrared Spectral Hole Burning of the SH Vibrational Mode in Hydrogenated As_2S_3 Glass," S. P. Love and A. J. Sievers, *Chemical Physics Letters* **153**, 379 (1988).
- \oplus "Determination of the orientation of NO_2^- in KI by persistent IR spectral hole burning," W. P. Ambrose and A. J. Sievers, *physica status solidi (b)* **151**, K97 (1989).

- "Zeeman Splitting of Double-Donor Spin-Triplet Levels in Silicon", R. E. Peale, R. M. Hart, A.J. Sievers and F. S. Ham, Proceedings of the Third International Conference on Shallow Impurities in Semiconductors, Institute of Physics Conference Series **95**, (1989).
- ⊕ "Observation of a Far-Infrared Sphere Resonance in Superconducting $\text{La}_{2-x}\text{Sr}_x\text{CuO}_{4-y}$ Particles," T. W. Noh, S. G. Kaplan and A. J. Sievers, Physical Review Letters **6**, 599 (1989).
 - ⊕ "Anharmonic Resonant Modes and the Low Temperature Specific Heat of Glasses," A. J. Sievers and S. Takeno, Physical Review B **39**, 3374 (1989).
- "Infrared Reflection-Absorption Spectroscopy of W(100)-H at 100 K," D. M. Riffe and A. J. Sievers, Surface Science **210**, L215 (1989).
- ⊕ "Far Infrared Difference Band Absorption in Potassium Iodide," S. P. Love, W. P. Ambrose and A. J. Sievers, Physical Review B **39**, 10 352 (1989).
 - ⊕ "Reply to comment on 'Observation of a far-infrared sphere resonance in superconducting $\text{La}_{2-x}\text{Sr}_x\text{CuO}_{4-y}$ '," T. W. Noh, S. G. Kaplan and A. J. Sievers, Physical Review Letters **62**, 2764 (1989).
 - ⊕ "The Near Millimeter Wave Properties of High Temperature Superconductors," A. J. Sievers, 16th Army Science Conference Proceedings Addenda, 25-27 October, (Dept. of the Army, 1988) p. 1-25.
- "On Antiferromagnetic Resonance in $\text{La}_2\text{CuO}_{4-y}$," S. G. Kaplan, T. W. Noh, A. J. Sievers, S-W. Cheong and Z. Fisk, Physical Review B **40**, 5190 (1989).
- "Comment on 'Relaxation-time enhancement in the heavy-fermion system CePd_3 '," P. E. Sulewski and A. J. Sievers, Physical Review Letters **63**, 2000 (1989).
- ⊕ "Far Infrared Sphere Resonance in Isolated Superconducting Particles," T. W. Noh, S. G. Kaplan and A. J. Sievers, Physical Review B **41**, 307 (1989).
 - ⊕ "Generalization of the Lyddane-Sachs-Teller relation to disordered dielectrics," T. W. Noh and A. J. Sievers, Physical Review Letters **63**, 1800 (1989).

- ⊕ "Investigation of the IR properties of ZnS:diamond composites," T. W. Noh, A. J. Sievers, L. A. Xue and R. Raj, *Optics Letters* **14**, 1260 (1989).
- ⊕ "Theoretical and Experimental Study of a Quantized Lattice Configuration in a Nearly Unstable Defect System," J. B. Page, J. T. McWhirter, A. J. Sievers, H. Fleurent, A. Bouwen and D. Schoemaker, *Phys. Rev. Lett.* **63**, 1837 (1989).
- ⊕ "Far Infrared Sphere Resonance in Isolated Superconducting Particles," T. W. Noh, S. G. Kaplan and A. J. Sievers, *Physical Review B* **41**, 307 (1990).
- ⊕ "Generalized Lyddane-Sachs-Teller Relation and Disordered Solids," A. J. Sievers and J. B. Page, *Physical Review B* **41**, 3455 (1990).

"Low Frequency Excitation Spectra of High T_c Superconductors," A. J. Sievers, T. W. Noh and S. G. Kaplan, *Phonons '89*, Proceedings of the Third International Conference on Phonon Physics, S. Hunklinger, W. Ludwig and G. Weiss, eds.(World Scientific, Singapore, 1990), Vol. 1, p. 237.

"Pulsed Laser Deposition of High T_c Superconducting Thin Films," S. E. Russek, B. H. Moeckly, R. A. Buhrman, J. T. McWhirter, A. J. Sievers, M. G. Norton, L. A. Tietz and B. Carter, *Materials Research Society Symposium Proceedings* **169**, 204, (1990).

"Hydrogen Adsorption on the β N covered W(100) Surface: An Infrared Study of the W-H Stretch," D. M. Riffe and A. J. Sievers, *Physical Review B* **41**, 3406 (1990).

"Infrared Diffuse Reflectivity Study of High T_c Superconductors," A. Rosenberg, A. S. Barker, T. W. Noh, T. Ohsaka and A. J. Sievers, *Physical Review B* **41**, 7213 (1990).

"IR study of (H,Be)-, (D,Be)- and (Li,Be)-acceptor complexes in silicon," R. E. Peale, K. Muro and A. J. Sievers, *Physical Review B* **41**, 5881 (1990).

"Far Infrared Absorption by Small Silver Particles in Gelatin," R. P. Devaty and A. J. Sievers, *Physical Review B* **41**, 7421 (1990).

- ⊕ "Persistent IR Spectral Hole Burning in Chalcogenide Glasses", S. P. Love and A. J. Sievers, *J. of Luminescence* **45**, 58 (1990).

- ⊕ "Optical and Mechanical Properties of Zinc Sulphide Diamond Composites," L. A. Xue, D. S. Farquar, R. Raj, T. W. Noh and A. J. Sievers, *Acta Metall. Mater.* **38**, 1743 (1990).
- ⊕ "On the Optical Response of a Disordered Solid with Restricted Size," A. J. Sievers and J. B. Page, *Physical Review B* **41**, 12 562 (1990).
- ⊕ "Persistent Infrared Spectral Hole Burning of Impurity Vibrational Modes in Chalcogenide Glasses", S. P. Love and A. J. Sievers, in *Transport, Correlation and Structural Defects*, Advances in Disordered Semiconductors, Vol. III, F. Fritzsche, ed., (World Scientific Publishing Co., Singapore, 1990), p. 27.
- ⊕ "Far IR Investigation of the Generalized Lyddane-Sachs-Teller Relation Using ZnS:diamond Composites," S. A. FitzGerald, T. W. Noh, A. J. Sievers, L. A. Xue and Y. Tzou, *Phys. Rev. B* **42**, 5469 (1990).
- ⊕ "Effect of Network Topology on Low Temperature Relaxation in Ge-As-Se Glasses as Probed By Persistent Infrared Spectral Hole Burning," S. P. Love, A. J. Sievers, B. L. Halfpap and S. M. Lindsay, *Phys. Rev. Lett.* **65**, 1792 (1990).
- ⊕ "Persistent Infrared Spectral Hole Burning," A. J. Sievers, *Optics and Photonics* **1**, No. 12, 53 (1990).
- ⊕ "IR Spectroscopic Study of the Dressed Rotations of CN⁻ isotopes in Alkali Halide Crystals," C. E. Mungan, R. C. Spitzer, J. P. Sethna and A. J. Sievers, *Phys. Rev. B* **43**, 43 (1991).
- ⊕ "Intrinsic Localized Modes in a Monatomic Lattice with Weakly Anharmonic Nearest Neighbor Force Constants," S. R. Bickham and A. J. Sievers, *Phys. Rev. B* **43**, 2339 (1991).
- ⊕ "A Generalized Lyddane-Sachs-Teller Relation for Solids and Liquids," A. J. Sievers and J. B. Page, *Infrared Physics* **32**, 425 (1991).
- ⊕ "Four-Wave Mixing in the Far Infrared from Free Carriers in n-type InSb," R. M. Hart, G. A. Rodríguez and A. J. Sievers, *Optics Letters*, Nov. (1991).

- ⊕ "Observation of Coherent Synchrotron Radiation at the Cornell Linac," E. B. Blum, U. Happek and A. J. Sievers, Nucl. Instrum. Methods Phys. Res., Sect. A, **307**, 568 (1991).
 - ⊕ "Prediction and Observation of Pocket Vibrational Modes in Crystals," K. W. Sandusky, J. B. Page, A. Rosenberg, C. E. Mungan and A. J. Sievers, Phys. Rev. Lett. **67**, 871 (1991).
 - ⊕ "Time Resolved Spectroscopy with Fourier Transform Spectrometers: Maintaining the Fellgett Advantage," J. T. McWhirter and A. J. Sievers, Applied Spectroscopy, Nov. (1991).
 - ⊕ "Persistent Infrared Spectral Hole Burning of NO_2^- Ions in Alkali Halide Crystals: I Principle and Satellite Hole Generation," W. P. Ambrose, J. P. Sethna and A. J. Sievers, J. Chem. Phys., Dec. 15 (1991).
- "Sulfur-Hydrogen Donor Complexes in Silicon", R. E. Peale, K. Muro, and A. J. Sievers, in Proceedings of the Fourth International Conference on Shallow Impurities in Semiconductors, Materials Science Forum, editor Gordon Davies (Trans Tech Publications, Switzerland, 1990) Vols. 65-66 pp. 151-156.
- ⊕ "Raman Scattering of KI:Ag^+ : Exploration of a Nearly Unstable Defect-Lattice Configuration," H. Fleurent, W. Joosen, J. B. Page, A. J. Sievers, J. T. McWhirter, A. Bouwen and D. Schoemaker, LATDIM '90
- "Self-Consistency Conditions for the Effective Medium Approximation in Composite Materials," T. W. Noh, P. H. Song and A. J. Sievers, Physical Review B **43** (1991).
- ⊕ "Observation of Coherent Transition Radiation," U. Happek, A. J. Sievers and E. B. Blum, submitted to Phys. Rev. Letters, (1991).
 - ⊕ "Persistent IR Hole Burning in Crystals and Glasses," A. J. Sievers, J. of Luminescence (1991).
 - ⊕ "Anomalous Relaxation of the SH^- Stretching Mode in Alkali Halides," U. Happek, C.E. Mungan, J.T. McWhirter, and A.J. Sievers, in preparation.

- ⊕ "Energy Transfer Between UV Generated Defects and IR Vibrational Modes of the CN⁻ Ion in Alkali Halide Crystals," J. T. McWhirter, U Happek and A. J. Sievers, in preparation.

Reports

- ⊕ "IR Emission from UV Irradiated Alkali Halide Crystals Containing Point Defects", J. T. McWhirter and A. J. Sievers, Bull. Amer. Phys. Soc. **34**, 993 (1989).
- ⊕ "KI:NO₂⁻ Gap Mode Assignments by Persistent IR Hole Burning and FIR Isotope Shifts", W.P. Ambrose and A.J. Sievers, Bull. Amer. Phys. Soc. **34**, 993 (1989).
- ⊕ "Persistent IR Spectral Hole Burning of Impurity Vibrational Modes in Chalcogenide Glasses", S. P. Love and A. J. Sievers, Bull. Amer. Phys. Soc. **34**, 1007 (1989).
- "Diffuse Infrared Reflectivity Study of Sintered YBa₂Cu₃O_{7-y}", A. Rosenberg, A. S. Barker, T. W. Noh and A.J. Sievers, Bull. Amer. Phys. Soc. **34**, 792 (1989).
- ⊕ "Magnetic Field Dependence of the Far Infrared Nonlinear Susceptibility of Free Carriers in n-InP", R. M. Hart, G. A. Rodriguez, S. A. FitzGerald, A. J. Sievers, Bull. Amer. Phys. Soc. **34**, 960 (1989).
- ⊕ invited paper: "Observation of a Far-Infrared Sphere Resonance in Superconducting La_{2-x}Sr_xCuO_{4-y} Particles", T. W. Noh, Bull. Amer. Phys. Soc. **34**, 791 (1989).
- "Far Infrared Transmission Measurements of YBa₂Cu₃O_{7-y} Thin Films", S. G. Kaplan, T. W. Noh, A. J. Sievers, S. E. Russek, and R. A. Buhrman, Bull. Amer. Phys. Soc. **34**, 792 (1989).
- ⊕ "Hot Carrier 2D Cyclotron Resonance Near the Intersubband Energy", G. A. Rodriguez, R. M. Hart, Z. Schlesinger and A. J. Sievers, Bull. Amer. Phys. Soc. **34**, 550 (1989).
- ⊕ "Persistent IR Spectral Hole Burning of Tb³⁺ in the Glass-like Mixed Crystal Ba_{1-x-y}La_xTb_yF_{2+x+y}", S. P. Love, A. J. Sievers and J. A. Campbell, Bull. Amer. Phys. Soc. **35**, 548 (1990).

- ⊕ "Four-Wave-Mixing in the Far Infrared From Free Carriers in n-InSb." G. A. Rodríguez, R. M. Hart, A. Rosenberg, and A. J. Sievers, *Bull. Amer. Phys. Soc.* **36**, 453 (1991).
- ⊕ "Energy Transfer Between UV Generated Defects and IR Vibrational Modes of the CN⁻ Ion in Alkali Halide Crystals." J. T. McWhirter, U Happek and A. J. Sievers, *Bull. Amer. Phys. Soc.* **36**, 841 (1991).
- ⊕ "Resonant Enhancement of Far Infrared Four-Wave-Mixing by Magnetoplasmons in n-InSb." R. M. Hart, G. A. Rodríguez and A. J. Sievers, *Bull. Amer. Phys. Soc.* **36**, 453 (1991).
- "Antiferromagnetic Resonance in R₂CuO₄." S. G. Kaplan, T. W. Noh, A. J. Sievers, S-W. Cheong, Z. Fisk, *Bull. Amer. Phys. Soc.* **36**, 881 (1991).
- ⊕ "Simulations of Intrinsic Localized Modes in a 2-D Anharmonic Lattice. S. R. Bickham and A. J. Sievers, *Bull. Amer. Phys. Soc.* **36**, 919 (1991).
- ⊕ "Vibrational Relaxation of Diatomic Molecular Defects: Saturation Experiments on HS⁻ in Alkali Halide Hosts." U. Happek, J.T. McWhirter, C.E. Mungan, and A.J. Sievers, *Bull. Amer. Phys. Soc.* **36**, 918 (1991).
- ⊕ "Isotope Dependence of IR Localized Modes of CN⁻ in Potassium Halide Crystals." C.E. Mungan, R.C. Spitzer, J.P. Sethna, A.J. Sievers, *Bull. Amer. Phys. Soc.* **36**, 842 (1991).
- ⊕ "Crystalline and Glass-like FIR Properties Exhibited by Mixed Crystals of (CaF₂)_{1-x}:(LaF₃)_x." S. A. Fitzgerald, T. W. Noh, J. A. Campbell, A. J. Sievers, *Bull. Amer. Phys. Soc.* **36**, 1022 (1991).
- ⊕ "Anomalous Isotope Effect for the Gap Mode in KI:Ag⁺, a Nearly Unstable Defect System." A. Rosenberg, C. E. Mungan and A. J. Sievers, *Bull. Amer. Phys. Soc.* **36**, 919 (1991).
- ⊕ (invited paper) "Persistent Infrared Spectral Hole Burning in Chalcogenide Glasses"—The Effects of Network Connectivity on Low-Temperature Relaxation. S. P. Love, *Bull. Amer. Phys. Soc.* **36**, 998 (1991).

Theses

"Adsorbates on W(100): Vibrational and Electronic Response in the IR," D. M. Riffe, Ph. D. Thesis, Cornell University (198).

- ⊕ "Persistent Infrared Spectral Hole Burning of Nitrite Ions in Alkali Halides," W. P. Ambrose, Ph. D. Thesis, Cornell University (1989).

"IR Studies of Chemical Splittings, Triplet Levels and Tunneling States at Electronic Defects in Silicon," R. E. Peale, Ph. D. Thesis, Cornell University (1990).

- ⊕ "Persistent Infrared Spectral Hole Burning Studies of Chalcogenide Glasses and Other Disordered Semiconductors," S. P. Love, Ph. D. Thesis, Cornell University (1991).

- ⊕ "Non-Resonant UV Pumping of IR Vibrational Fluorescence from CN^- in Alkali Halides," J. T. McWhirter, Ph. D. Thesis, Cornell University (1991).

- ⊕ "Intensity Dependent Cyclotron Resonance in a GaAs:AlGaAs Two Dimensional Electron Gas," Gerardo Rodriguez, Ph. D. Thesis, Cornell University (1991).

- ⊕ "Nonlinear Magneto-optics of Semiconductors in the Far Infrared," R. M. Hart, Ph. D. Thesis, Cornell University (1991).

G. Participating scientific personnel

S. R. Bickham, graduate student

J. T. McWhirter, graduate student

C. E. Mungan, graduate student

W. P. Ambrose, graduate student

S. P. Love, graduate student

A. Rosenberg, graduate student

Gerardo Rodriguez, graduate student

R. M. Hart, graduate student

Dr. T. W. Noh, postdoc

Dr. Uwe Happek, postdoc

Dr. J. A. Campbell, visiting scientist

Professor A. S. Barker, visiting Professor

III. REFERENCES

1. J. T. McWhirter and A. J. Sievers, *Bull. Amer. Phys. Soc.* **34**, 993 (1989).
2. J. T. McWhirter, Ph. D. Thesis, Cornell University (1991).
3. F. Lüty, *Cryst. Latt. Def. and Amorph. Mat.* **12**, 343 (1985).
4. T. R. Gosnell, R. W. Tkach and A. J. Sievers, *Infrared Phys.* **25**, 35 (1985).
5. J. D'Hertoghe and G. Jacobs, *phys. stat. sol. b* **95**, 291 (1979).
6. F. Lüty, *Z. Physik* **160**, 1 (1960).
7. M. N. Kabler, in *Point Defects in Solids*, edited by James H. Crawford and L. M. Slifkin, (Plenum Press, N.Y., 1972), Vol. 1, Ch. 6.
8. Y. Yang and F. Lüty, *Phys. Rev. Lett.* **51**, 419 (1983).
9. J.J. Sloan and E.J. Kruus, in *Time Resolved Spectroscopy*, R.J.H. Clark and R.E. Hester, editors., John Wiley and Sons, 1989, Ch. 5.
10. A. Laubereau and M. Stockberger, in *Time-resolved Vibrational Spectroscopy*, Springer Proceedings in Physics, (Springer, Berlin, 1985).
11. P. Fellgett, *J. Phys. Radium* **19**, 187 (1958).
12. P. Jacquinot, *Rep. Prog. Phys.* **23**, 267 (1960).
13. J. T. McWhirter and A. J. Sievers, *Applied Spectroscopy*, Nov. (1991).
14. P. R. Griffiths and J. A. de Haseth, *Fourier Transform Infrared Spectroscopy*, (John Wiley and Sons, NY, 1986), Ch. 4.
15. T. R. Fletcher and S. R. Leone, *J. Chem. Phys.* **88**, 4720 1988.
16. Henri Buijs, BOMEM Inc., Private communication
17. J. Manz, *J. Amer. Chem. Soc.* **102**, 1801 (1980).
18. H. Dubost, *Chem. Phys.* **12**, 139 (1976).
19. T. R. Gosnell, R. W. Tkach and A. J. Sievers, *J. of Lumin.* **31-32**, 166 (1984).
20. K.P. Koch, Y. Yang, and F. Lüty, *Phys. Rev. B* **29**, 5840 (1984).
21. J.B. Page and B.G. Dick, *Phys. Rev.* **163**, 910 (1967).
22. U. Happek, C.E. Mungan, J.T. McWhirter, and A.J. Sievers, to be published.
23. C.-K. Chi and E.R. Nixon, *J. Phys. Chem. Solids* **33**, 2101 (1972).
24. See for example R. Loudon, *The Quantum Theory of Light*, 2nd ed. (Oxford, Clarendon Press, 1990), Chap. 1, especially Eq. (1.100).
25. H. Graener, G. Seifert and A. Laubereau, *Chem. Phys. Lett.* **172**, 435 (1990).
26. H. J. Bakker et al., *J. Chem. Phys.* **94**, 1730 (1991).

27. R. O. Pohl, in *Amorphous Solids: Low Temperature Properties*, edited by W. A. Phillips (Springer -Verlag, Berlin, 1981), p.37.
28. A. J. Sievers and S. Takeno, *Phys. Rev. Letters* **61**, 970 (1988).
29. S. Takeno, K. Kisoda and A. J. Sievers, *Progress in Theoretical Physics, Supplement* **94**, 242 (1988).
30. J. B. Page, *Phys. Rev. B* **41**, 7835 (1990).
31. R. Bourbonnais and R. Maynard, *Phys. Rev. Lett.* **64**, 1397 (1990).
32. V. M. Burlakov, S. A. Kiselev and V. N. Pyrkov, *Solid State Commun.* **74**, 327 (1990).
33. V. M. Burlakov, S. A. Kiselev and V. N. Pyrkov, *Phys. Rev. B* **42**, 4921 (1990).
34. S. Takeno and K. Hori, *J. Phys. Soc. Japan* **59**, 3037 (1990).
35. S. R. Bickham and A. J. Sievers, *Phys. Rev. B* **43** (1991).
36. H. Shechter, E. A. Stern, Y. Yacoby, R. Brener, and Zhe Zhang, *Phys. Rev. Lett.* **63**, 1400 (1989).
37. J. B. Page, J. T. McWhirter, A. J. Sievers, H. Fleurent, A. Bouwen and D. Schoemaker, *Phys. Rev. Lett.* **63**, 1837 (1989).